J. Membrane Biol. 86, 203–210 (1985)

The Journal of
Membrane Biology

Water Permeability of *Necturus* Gallbladder Epithelial Cell Membranes Measured by Nuclear Magnetic Resonance

Martin C. Steward and Mary J. Garson*
Department of Physiology, University of Manchester, Manchester, M13 9PT, United Kingdom
and University Chemical Laboratories, Cambridge, CB2 1EW, United Kingdom

Summary. In order to assess the contribution of transcellular water flow to isosmotic fluid transport across *Necturus* gallbladder epithelium, we have measured the water permeability of the epithelial cell membranes using a nuclear magnetic resonance method. Spin-lattice (T_1) relaxation of water protons in samples of gallbladder tissue where the extracellular fluid contained 10 to 20 mM Mn^{2+} showed two exponential components. The fraction of the total water population responsible for the slower of the two was 24 ± 2%. Both the size of the slow component, and the fact that it disappeared when the epithelial layer was removed from the tissue, suggest that it was due to water efflux from the epithelial cells. The rate constant of efflux was estimated to be 15.6 ± 1.0 sec^{-1} which would be consistent with a diffusive membrane water permeability P_d of 1.6×10^{-3} cm sec^{-1} and an osmotic permeability P_{os} of between 0.3×10^{-4} and 1.4×10^{-4} cm sec^{-1} $osmolar^{-1}$. Using these data and a modified version of the standing-gradient model, we have reassessed the adequacy of a fluid transport theory based purely on transcellular osmotic water flow. We find that the model accounts satisfactorily for near-isosmotic fluid transport by the unilateral gallbladder preparation, but a substantial serosal diffusion barrier has to be included in order to account for the transport of fluid against opposing osmotic gradients.

Key Words *Necturus* gallbladder · water permeability · nuclear magnetic resonance · standing-gradient model · isosmotic fluid transport

Introduction

The continuing uncertainty about the route of water transport across leaky epithelia such as the gallbladder has been attributed to a lack of information about the osmotic permeability (P_{os}) of the epithelial cell membranes (Diamond, 1979; Hill, 1980; Spring & Ericson, 1982). It has been argued that the P_{os} of these membranes must be unusually large if transcellular osmosis is to account for fluid transport (Hill, 1975), but until recently the only available measurements of P_{os} have been those obtained from whole epithelia (e.g. van Os et al., 1979) rather than from the cell membranes. Values of P_{os} for the cell membranes are, however, essential for any rigorous assessment of fluid transport models based on transcellular osmosis and, for various reasons, they cannot easily be deduced from transepithelial water flow measurements.

Persson and Spring (1982) have addressed the problem more directly by measuring rates of change of cell volume in *Necturus* gallbladder when the epithelium is exposed to step changes in extracellular osmolarity. Their results do not reveal unusually large values for P_{os} but the authors claim that, in the context of a simple two-barrier model, the figures are nonetheless sufficient to account for the near-isotonicity of fluid transport.

Inevitably, the cell volume technique displays some technical limitations and poses problems of interpretation. Not the least of these are the uncertainty about the influence of unstirred layer effects, and, owing to the leakiness of the paracellular pathway, the difficulty of applying step changes in osmolarity separately to the apical and basolateral membranes. We have therefore explored the use of a totally different technique which, though it measures diffusive water permeability, P_d, rather than P_{os}, nonetheless provides an order-of-magnitude estimate of the latter. Furthermore, it has the advantage that the measurement is made at equilibrium thus obviating any uncertainty about unstirred layer effects. The method is based on a nuclear magnetic resonance (NMR) relaxation technique which has already been used with success to determine the P_d of erythrocyte membranes (Fabry & Eisenstadt, 1975). In outline, the method measures the rate constant of diffusive water efflux from the cell interior, where water proton relaxation is very slow, to the extracellular fluid, where relaxation is

* *Present address:* Sir George Fisher Centre for Tropical Marine Studies, James Cook University of North Queensland, Australia.

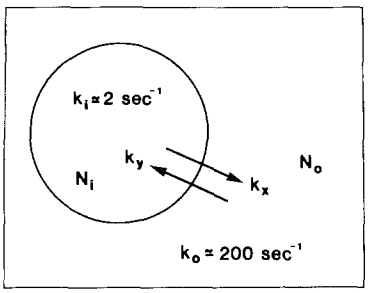

Fig. 1. Rate constants of spin-lattice relaxation (k_i, k_o) and diffusive exchange (k_x, k_y) between intracellular and extracellular water molecule populations (N_i, N_o). Based on Fabry and Eisenstadt (1978)

accelerated by a factor of about 100 by the presence of a low concentration of Mn^{2+} ions.

In this initial study, we have concentrated on determining a mean permeability for the whole cell surface rather than attempting to measure separately the apical and basolateral permeabilities. The results obtained have been used to reassess the adequacy of fluid transport models based on osmotic water flow via a transcellular route.

Materials and Methods

Adult *Necturus maculosus* were obtained from Xenopus Ltd. (Redhill, Surrey, UK) and kept at room temperature in a running-water aquarium. They were anesthetized by immersion in a 1% urethane solution and pithed prior to dissection. Gallbladders were removed, emptied and cut open, and then rinsed with an oxygenated HCO_3^--free Ringer's solution of the following composition (mM): 100 NaCl, 2.5 KCl, 1 $CaCl_2$ and 10 Tris buffer (pH 7.4). Each sample prepared for the NMR measurements consisted of three gallbladders; these were bathed for about 10 min in a Ringer's solution in which some of the NaCl was isosmotically replaced by 10, 15 or 20 mM $MnCl_2$. The Mn^{2+} ions had access to both surfaces of the epithelium. After soaking in the Mn^{2+} solution, the three pieces were swabbed with moistened filter paper and packed loosely into a small glass sample tube together with a sealed glass capillary containing D_2O. The sample tube was then placed at the bottom of a standard 5 mm NMR tube. The tissue sample occupied a height of approximately 5 mm.

In two experiments, the epithelial cell layer was separated from the rest of the gallbladder wall and discarded before soaking the latter alone in the Mn^{2+} solution. Separation was achieved by pinning the gallbladder as a flat sheet onto a Sylgard® resin surface (Dow Corning Corporation, Midland, Mich.) under oxygenated Ringer's solution, and then peeling the epithelium away from the subepithelial tissue with a scalpel blade and fine watchmaker's forceps. In one further experiment, the sample consisted of flakes of epithelium which had been obtained in the same way and suspended in a small volume of Ringer's solution containing 5 mM Mn^{2+}.

NMR Measurements

Measurements were made at 100 MHz on a Varian XL100-A spectrometer using an external D_2O lock. The spin-lattice (T_1) relaxation of the water protons in the samples was assessed by a standard inversion-recovery pulse sequence (Farrar & Becker, 1971). A 180° pulse inverted the net magnetization and its recovery was monitored by applying a 90° test pulse after a known delay, t. The amplitude of the resulting free induction decay was measured as a function of the delay time, the latter being varied between 0.001 and 5 sec. Results are presented as the difference between the net magnetization after a delay of t sec, $M(t)$, and the equilibrium value as estimated from the magnetization existing after a delay of 5 or 10 sec, $M(\infty)$, the difference being normalized to unity at zero time.

Data Analysis

The kinetics of spin-lattice relaxation in a two-compartment system where there is exchange between the compartments has been described in detail elsewhere (Woessner, 1961; Fabry & Eisenstadt, 1975, 1978). In the present application, inclusion of a low concentration of paramagnetic Mn^{2+} ions in the extracellular compartment enhances the relaxation process in that compartment so that the relaxation time constant, T_1, for water protons is reduced from about 2 sec to 5 msec. Inside the cell, the water protons are assumed to be uninfluenced by the extracellular Mn^{2+} ions and the relaxation process is much slower with a T_1 of approximately 0.5 sec.

If there were no exchange between the compartments, the total net magnetization would decay after an inverting pulse according to the sum of two exponentials whose rate constants would simply reflect the T_1 values in the two compartments. If, however, the water molecules are free to move between the two compartments by diffusion, and are leaving the cellular compartment with a rate constant k_x that lies between the cellular and extracellular relaxation rate constants, the rate constant of the slower exponential will become dominated by k_x.

More precisely, if the deviation of intracellular and extracellular magnetization from their equilibrium values are M_i and M_o, respectively, the relaxation process is described by

$$\frac{dM_i}{dt} = -(k_i + k_x)M_i + k_y M_o \quad (1)$$

$$\frac{dM_o}{dt} = -(k_o + k_y)M_o + k_x M_i \quad (2)$$

where k_i and k_o are the relaxation rate constants ($1/T_1$) inside and outside the cells, and k_x and k_y are the rate constants for water efflux and influx across the cell membrane (*see* Fig. 1).

At equilibrium, water efflux equals water influx and thus

$$k_x N_i = k_y N_o \quad (3)$$

where N_i and N_o are the total amounts of exchangeable water in the two compartments.

The quantity measured in the NMR experiment is $M_i + M_o$. The expression obtained for $M_i + M_o$ from the general solution of Eqs. (1) and (2) and normalized to unity at zero time is

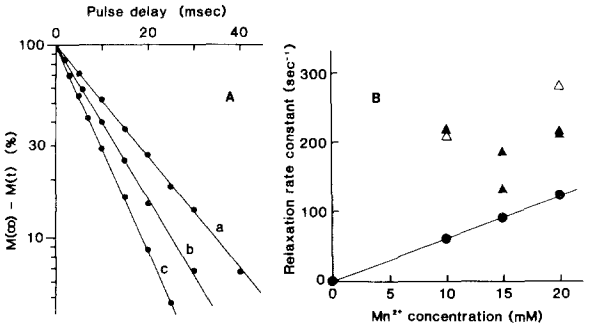

Fig. 2. (*A*) Spin-lattice relaxation of water protons in samples of Ringer's solution containing three different Mn^{2+} concentrations: *a*, 10 mM; *b*, 15 mM; *c*, 20 mM. (*B*) Relationship between relaxation rate constant ($1/T_1$) and Mn^{2+} concentration in Ringer's solution samples (●), and between the derived rate constant k_o and extracellular Mn^{2+} concentration in whole gallbladders (▲) and gallbladders from which the epithelia had been removed (△)

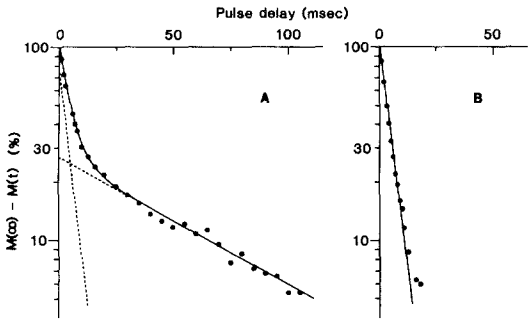

Fig. 3. Spin-lattice relaxation of water protons in samples consisting of: *A*, three intact gallbladders (ϕ_A = 219 sec^{-1}, ϕ_B = 15.1 sec^{-1} and H = 26.9%); *B*, three gallbladders after removal of their epithelia (ϕ_A = 211 sec^{-1}). The extracellular Mn^{2+} concentration was 10 mM in both cases. ϕ_A and ϕ_B are the rate constants of the faster and slower exponential components and H is the zero-time intercept of the slower component

$$M_i + M_o = (1 - H)\exp(-\phi_A t) + H\exp(-\phi_B t) \quad (4)$$

where the rate constants ϕ_A and ϕ_B are given by

$$\phi_A = \tfrac{1}{2}(k_i + k_o + k_x + k_y) + \tfrac{1}{2}\sqrt{(k_i - k_o + k_x - k_y)^2 + 4k_xk_y} \quad (5)$$

$$\phi_B = \tfrac{1}{2}(k_i + k_o + k_x + k_y) - \tfrac{1}{2}\sqrt{(k_i - k_o + k_x - k_y)^2 + 4k_xk_y}. \quad (6)$$

The zero-time intercept H of the slow component is related to the intracellular fraction f_i of the total water molecule population according to

$$H = \frac{f_i(k_o - k_i) + \phi_A - k_o}{\phi_A - \phi_B} \quad (7)$$

where

$$f_i = N_i/(N_i + N_o). \quad (8)$$

An approximate solution which can be shown to hold under the conditions of these experiments, where $k_i \ll k_x$ and $k_y \ll k_o$, is

$$\phi_A \approx k_o + k_y \quad (9)$$

$$\phi_B \approx k_i + k_x. \quad (10)$$

In the present study, the rate constants ϕ_A and ϕ_B and the zero-time intercept H were estimated from the experimental data by least-squares curve-fitting using the nonlinear regression routine in the SPSS library as implemented at the University of Manchester Regional Computing Centre. Values for k_x and P_i which satisfy Eqs. (3) and (7) to (10) were obtained by iteration.

Results

Mn^{2+}-Ringer's Solutions

In a series of control experiments, the T_1 relaxation of small samples of Ringer's solution containing various concentrations of Mn^{2+} ions consistently followed a simple exponential decay. In every case, a log-linear plot of the deviation of net magnetization $M(t)$ from its equilibrium value $M(\infty)$ against pulse delay t was fitted well by a straight line over the two measurable decades of relaxation (Fig. 2*A*). As shown by Fig. 2*B*, the rate constant of relaxation $1/T_1$ obtained from the slope of these lines was approximately linearly related to the Mn^{2+} concentration up to 20 mM.

Intact Tissue Samples

Relaxation data obtained in exactly the same way from samples consisting of three emptied gallbladders presoaked in a Mn^{2+}-Ringer's solution were more complex. Figure 3*A* shows the results from one such sample. As expected of a two-compartment system, the relaxation time-course is dominated by two exponential components. Values for the rate constants of the two components, ϕ_A and ϕ_B, and the zero-time intercept of the slow component H have been obtained by least-squares curve-fitting and are listed in Table 1 together with the results from four similar samples soaked in various external Mn^{2+} concentrations. In each case, sufficient data were obtained at the longer pulse delays

Table 1. Rate constants and relative magnitude of the fast and slow components of spin-lattice relaxation[a]

Sample number	$[Mn^{2+}]$ (mM)	ϕ_A (sec^{-1})	ϕ_B (sec^{-1})	H (%)
(a) Intact epithelium				
1	20	214 ± 21	19.8 ± 3.5	22.3 ± 3.2
2	20	220 ± 26	19.3 ± 2.3	32.9 ± 3.3
3	15	136 ± 11	15.3 ± 1.1	34.9 ± 2.5
4	15	188 ± 13	18.4 ± 1.8	25.2 ± 2.3
5	10	219 ± 14	15.1 ± 1.0	26.9 ± 1.5
(b) Epithelium removed				
6	20	281 ± 32	—	—
7	10	211 ± 17	—	—

[a] Curve-fit parameters are listed with their 95% confidence limits.

for the time-course of the slow-component and the zero-time intercept to be defined with reasonable precision.

Using the expressions given in the Materials and Methods section for the kinetics of a two-compartment system with exchange, the measured values of ϕ_A, ϕ_B and H have been used to estimate: (i) the rate constants of exchange k_x and k_y; (ii) the rate constant of relaxation in the extracellular fluid k_o; and (iii) the size of the exchangeable intracellular water pool f_i expressed as a fraction of the total water content of the sample. The calculations require an estimate of the relaxation rate constant of the intracellular water protons k_i, which proved inaccessible to measurement in this tissue since most of the water proton signal derives from extracellular water and we were unable to obtain samples of higher cytocrit. However, T_1 values for cell water in the literature invariably lie close to 500 msec (Mathur-De Vré, 1979) and a value of 0.002 $msec^{-1}$ has therefore been assumed in the present calculations. Increasing or decreasing this figure by a factor of two, the maximum error that is likely to have been introduced by assuming this value, makes little significant difference to the calculated values of the other kinetic parameters.

The rate constant of water proton relaxation in the extracellular fluid k_o which largely defines the rate constant of the fast component of relaxation ϕ_A surprisingly showed little correlation with the extracellular Mn^{2+} concentration (Fig. 2*B*).The values of k_0 were also consistently faster than the rate constants obtained from samples of Mn^{2+}-Ringer's solution alone. Taken together, these two observations suggest that association of the Mn^{2+} ions with the tissue had maximized their capacity to enhance relaxation.

Assuming a value of 2 sec^{-1} for k_i, the mean values of the exchange rate constants k_x and k_y obtained in the five sets of data were 15.6 ± 1.0 sec^{-1} and 4.9 ± 0.5 sec^{-1}, respectively. The exchangeable intracellular water pool accounted for 24.1 ± 1.9% of the total signal.

Removal of the Epithelium

In order to establish whether the slow component really reflects water efflux from the cellular compartment, an attempt was made to separate the epithelial layer from the remainder of the gallbladder wall by dissection. This proved easy and samples consisting of three gallbladders, with their epithelia removed, were soaked in Mn^{2+}-Ringer's solutions and relaxation data obtained as before.

Data obtained from one such sample are illustrated in Fig. 3*B*, and, unlike those from the intact sample (Fig. 3*A*), they are fitted satisfactorily by a single exponential. Furthermore, the rate constant of this single component is indistinguishable from the fast-component rate constant ϕ_A obtained from the intact tissue samples (Table 1). This indicates that the presence of the slow component is certainly dependent on the presence of the epithelium. It is also interesting to note that the relaxation enhancement due to the Mn^{2+} ions is still greater than that seen with the Mn^{2+}-Ringer's solution alone (Fig. 2*B*), even in the absence of the epithelium. This suggests that the association of Mn^{2+} ions with the tissue occurs in the nonepithelial regions, although association with the epithelium as well in the intact preparation cannot be excluded.

Attempts to determine the relaxation kinetics of water protons in pieces of isolated epithelium suspended in Mn^{2+}-Ringer's solution proved less successful. Despite very careful handling, the epithelial pieces broke into 'flakes' and single cells during preparation, and this was paralleled by a loss of viability as assessed by trypan blue exclusion in a 0.02% solution. In the NMR probe, the spinning of the sample tube and the presence of the D_2O capillary insert probably accelerated the disintegration of the epithelium, and unlike all the other samples examined, the relaxation time-course changed with time over the course of the measurements. The slow component, although most certainly present during the first 30 min, gradually disappeared or, more probably, its time constant decreased, over the course of the following hour as shown by the data in Fig. 4.

Discussion

The data obtained in this study suggest that, at equilibrium, water molecules diffuse out of the epithelial cells of *Necturus* gallbladder with a rate constant of approximately 16 sec^{-1}. This is a 'lumped' figure which does not distinguish between water movement across the apical and basolateral membranes. Its accuracy is inevitably subject to several possible sources of error. For example, Mn^{2+} may itself have altered the membrane water permeability. Unpublished results from this laboratory suggest, however, that transepithelial ^{3}H-water permeability measured in perfused sac preparations is little changed by the presence of Mn^{2+} at the concentrations used in the NMR experiments. Mean values of the transepithelial permeability, although severely distorted by unstirred layer effects, decreased from $1.33 \pm 0.25 \times 10^{-4}$ cm sec^{-1} ($n = 4$) in normal Ringer's solution to $1.26 \pm 0.29 \times 10^{-4}$ cm sec^{-1} ($n = 4$) in 10 mM Mn^{2+} Ringer's and 1.22×10^{-4} cm sec^{-1} ($n = 2$) in 20 mM Mn^{2+} Ringer's. Another possibility is that Mn^{2+} ions distorted the NMR results by entering the cells during the experiment. The absence of any significant drift in the relaxation data over periods of up to 2 hr suggests that this effect was also minimal.

Our belief that the slow component of water proton relaxation reflects water efflux from the epithelial cells rests on two principal observations. First, the size of the water compartment contributing this component of the signal, 24% of the total water content of the sample, is compatible with the histology of the *Necturus* gallbladder where the epithelium occupies approximately one quarter of the total tissue thickness. Second, selective removal of the epithelium by dissection resulted in the total disappearance of the slow component. We therefore feel confident that k_x represents a reasonable estimate of the rate constant of water efflux from the epithelial cells.

Diffusive Water Permeability P_d

To translate the efflux rate constant k_x into a diffusive permeability coefficient P_d (House, 1974), we require information about the surface area and volume of the epithelial cells. Spring and Hope (1979) have used an optical technique to measure both of these parameters. After correction for refractive index (Persson & Spring, 1982), their average value for the volume of a *Necturus* gallbladder epithelial cell is approximately 20,500 μm^3, and the gross apical and basolateral areas (neglecting microvilli and lateral membrane folds) are 600 and 3,900 μm^2, respectively. Without stereological data for the surface amplification factors in this epithelium, it is difficult to estimate the true apical and basolateral membrane areas. However, Suzuki et al. (1982) have measured the apical and basolateral membrane capacitances in *Necturus* gallbladder. On the assumption that, like most biological membranes, the capacitance per unit area of the epithelial cell membrane is 1 $\mu F\ cm^{-2}$, their data indicate that the apparent apical area is amplified approximately eightfold by the presence of microvilli, and that membrane folds increase the apparent basolateral area approximately fourfold.

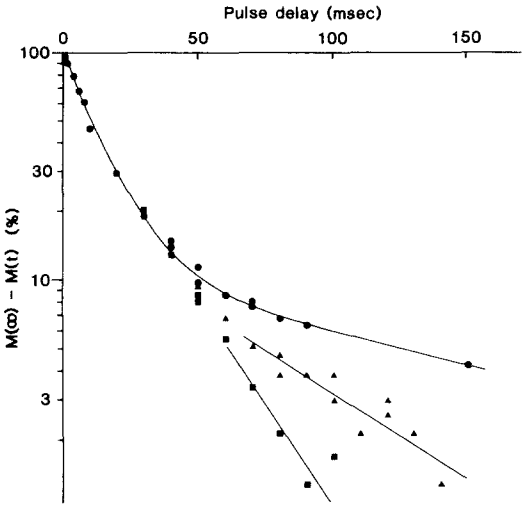

Fig. 4. Spin-lattice relaxation of water protons in a sample consisting of isolated epithelial flakes suspended in a small volume of Ringer's solution containing 5 mM Mn^{2+}. Data obtained within the first 30 min after dissection (●) are fitted well by a double exponential function where $\phi_A = 77\ sec^{-1}$, $\phi_B = 6.7\ sec^{-1}$ and $H = 11.0\%$. Data collected after further intervals of approximately 30 min (▲) and 60 min (■) show a progressive decline in the time constant of the slow component

The total membrane area of each epithelial cell thus appears to be around 20,400 μm^2, and consequently the volume/area ratio (V/A) is approximately 1.0×10^{-4} cm. Thus, using the relationship:

$$P_d = k_x \cdot V/A \qquad (11)$$

we obtain a diffusive permeability for the epithelial cell membranes of 1.6×10^{-3} cm sec^{-1}. This figure lies well within the range of values characteristic of animal cell membranes (House, 1974) and close to values obtained for artificial phospholipid membranes (reviewed by Fettiplace & Haydon, 1980). It is somewhat smaller than the P_d of the mammalian

erythrocyte which generally lies in the range of 4×10^{-3} to 6×10^{-3} cm sec^{-1} (House, 1974). Thus there is nothing in our results to suggest that the epithelial cell membranes of *Necturus* gallbladder have an uncommonly high P_d.

Osmotic Water Permeability P_f

The relationship between osmotic permeability P_f and diffusive permeability P_d has been discussed in detail elsewhere (e.g. House, 1974; Hill, 1979; Fettiplace & Haydon, 1980). In outline, P_f is expected to equal P_d in a nonporous membrane where osmotic water flow is necessarily diffusive in nature, but P_f will exceed P_d in a porous membrane where there is the possibility of viscous flow. The ratio P_f/P_d declines towards 1, however, as pore radius decreases and diffusive flow increasingly predominates. Exceptions to this latter rule occur when water flow through long, narrow pores involves a single-file process. Under these circumstances, P_f/P_d is believed to be approximately equal to the average number of water molecules inside the pore (Rosenberg & Finkelstein, 1978) and could exceptionally be as high as 10.

Since our aim is to estimate osmotic permeability, a value has to be assumed for P_f/P_d. If the gallbladder cell membranes are porous, the pores are unlikely to be large in diameter because, for osmotic water flow to be driven efficiently by solute gradients, the pores must be small enough to exclude the solutes. On the other hand, small pores might well show single-file properties and P_f/P_d could be as high as 5 if, for example, the pores resembled an antibiotic channel such as gramicidin A (Rosenberg & Finkelstein, 1978). Allowing for this possibility, we might expect P_f/P_d to lie somewhere between 1 and 5.

We conclude, therefore, that the value of P_f for the *Necturus* gallbladder cell membranes, after correction for membrane convolution, most probably lies between 1.6×10^{-3} and 8.0×10^{-3} cm sec^{-1}. Persson and Spring (1982), using a totally different technique, have obtained data describing the swelling and shrinkage of *Necturus* gallbladder cells in response to osmotic gradients, and their P_f values for the apical and basolateral membranes are 4.6×10^{-3} and 6.8×10^{-3} cm sec^{-1}.

For the purposes of modelling osmotic flow across the epithelium, it is more convenient to express the osmotic permeability in units of cm sec^{-1} osmolar^{-1}. To avoid confusion, this parameter is denoted P_{os} and it is related to P_f according to

$$P_{os} = P_f \cdot \bar{V}_w \cdot 10^{-3} \qquad (12)$$

where $\bar{V}_w$ is the partial molar volume of water (18 cm^3 mol^{-1}). Our estimate of P_{os}, therefore, lies between 0.3×10^{-4} and 1.4×10^{-4} cm sec^{-1} osmolar^{-1}. An order-of-magnitude estimate of 10^{-4} cm sec^{-1} osmolar^{-1} will be used in the remainder of this discussion. We have, incidentally, assumed in our calculation that the membranes of the apical and basolateral surfaces of the cells are identical with respect to their water permeability properties. This may well not be true, but the similarity of the apical and basolateral P_f values given by Spring (1983) suggests that it is a reasonable approximation.

The effective P_{os} of the apical surface of the cell is, of course, enhanced by the presence of microvilli. As mentioned above, these provide a surface amplification factor of about 8, so we expect the apical P_{os} to be effectively 8×10^{-4} cm sec^{-1} osmolar^{-1}. The amplification factor due to the folding of the basolateral membrane is about 4, so the effective P_{os} there will be about 4×10^{-4} cm sec^{-1} osmolar^{-1}.

Isosmotic Fluid Transport

It has been argued (Hill, 1975) that for the standing-gradient model of fluid absorption (Diamond & Bossert, 1967) to account adequately for experimental observation, the water permeability of the epithelial cell membranes would have to be unreasonably high. This conclusion resulted in part from the fact that, as Sackin and Boulpaep (1975) pointed out, the original standing-gradient model included a physically unrealistic boundary condition. Diamond and Bossert made it a requirement that the interspace fluid at the serosal end of the interspace be *exactly* isosmotic with the cell interior. By replacing this requirement with the more realistic condition that the osmolarity of the interspace fluid at the serosal end will be equal to the serosal bath osmolarity, the demands on P_{os} ease dramatically.

Taking a very simple standing-gradient model (described in outline in the Appendix and illustrated in Fig. 5), it is easy to show that near-isosmotic fluid transport by the *Necturus* gallbladder is accounted for satisfactorily by transcellular osmosis—at least in the case of the unilateral or 'sweating' preparation. Using the modest osmotic permeabilities obtained in this study, the modified standing-gradient model predicts that a unilateral sac preparation filled with a 200 mosmolar Ringer's solution would generate an absorbate with an osmolarity of 204 mosmolar—compatible with experimental observation. The steepness of the standing gradient in the interspace under these circumstances would, we calculate, be infinitesimally small—in accordance

with the predictions of Sackin and Boulpaep (1975) and Weinstein and Stephenson (1981)—and the system is therefore well approximated by the two-barrier model of Persson and Spring (1982).

One situation where the simple standing-gradient model and the two-barrier model fail to account for observation is the case where the gallbladder is bathed on both sides by the same solution. In the rabbit, and probably also *Necturus*, fluid absorption continues to be near-isosmotic under these conditions (Whitlock & Wheeler, 1964), but the standing-gradient model predicts a 1600 mosmolar absorbate, and the two-barrier model predicts zero volume flow. Likewise, both models fail to account for the ability of the gallbladder epithelium to transport fluid against osmotic gradients—up to 20 mosmolar in the case of *Necturus* (Persson & Spring, 1982). However, as Weinstein and Stephenson (1981) have shown, this experimental observation can be mimicked satisfactorily if a solute diffusion barrier is included between the interspace and the serosal bath. This could be the basement membrane and/or the connective tissue layers of the gallbladder wall. By adding a basement membrane to the model described in the Appendix, we calculate that its NaCl permeability would need to be approximately 2.6×10^{-5} cm sec^{-1} (equivalent to about 50 ohm cm^2) in order to account for a 'strength of transport' (Weinstein & Stephenson, 1981) of 20 mosmolar. It would simultaneously reduce the expected absorbate osmolarity of the symmetrically bathed epithelium from 1600 to 244 mosmolar, and it would have no effect on the absorbate osmolarity expected from the unilateral preparation. The existence of this barrier and its precise location and permeability characteristics, however, remain to be established.

This work was supported by the Medical Research Council (UK) and by New Hall, Cambridge, UK. We thank Prof. B.Z. Ginzburg for instigating this study, Prof. R. Raphael and Prof. R.D. Keynes for generously providing laboratory facilities, and Drs. A.E. and B.S. Hill, Dr. I.D. Campbell and Prof. R.M. Case for helpful discussions.

References

Diamond, J.M. 1979. Osmotic water flow in leaky epithelia. *J. Membrane Biol.* **51:**195–216

Diamond, J.M., Bossert, W.H. 1967. Standing-gradient osmotic flow. A mechanism for coupling of water and solute transport in epithelia. *J. Gen. Physiol.* **50:**2061–2083

Fabry, M.E., Eisenstadt, M. 1975. Water exchange between red cells and plasma. Measurement by nuclear magnetic relaxation. *Biophys. J.* **15:**1101–1110

Fabry, M.E., Eisenstadt, M. 1978. Water exchange across red cell membranes: II. Measurement by nuclear magnetic resonance T_1, T_2, and T_{12} hybrid relaxation. The effects of osmolarity, cell volume, and medium. *J. Membrane Biol.* **42:**375–398

Farrar, T.C., Becker, E.D. 1971. Pulse and Fourier Transform NMR. Academic, New York

Fettiplace, R., Haydon, D.A. 1980. Water permeability of lipid membranes. *Physiol. Rev.* **60:**510–550

Hill, A.E. 1975. Solute-solvent coupling in epithelia: A critical examination of the standing-gradient osmotic flow theory. *Proc. R. Soc. London B* **190:**99–114

Hill, A.E. 1979. Osmosis. *Q. Rev. Biophys.* **12:**67–99

Hill, A.E. 1980. Salt-water coupling in leaky epithelia. *J. Membrane Biol.* **56:**177–182

Hill, A.E., Hill, B.S. 1978. Sucrose fluxes and junctional water flow across *Necturus* gall bladder epithelium. *Proc. R. Soc. London B* **200:**163–174

House, C.R. 1974. Water Transport in Cells and Tissues. Arnold, London

Mathur-De Vré, R. 1979. The NMR studies of water in biological systems. *Prog. Biophys. Mol. Biol.* **35:**103–134

Os, C.H. van, Wiedner, G., Wright, E.M. 1979. Volume flows across gallbladder epithelium induced by small hydrostatic and osmotic gradients. *J. Membrane Biol.* **49:**1–20

Persson, B.-E., Spring, K.R. 1982. Gallbladder epithelial cell hydraulic water permeability and volume regulation. *J. Gen. Physiol.* **79:**481–505

Rosenberg, P.A., Finkelstein, A. 1978. Water permeability of gramicidin A-treated lipid bilayer membranes. *J. Gen. Physiol.* **72:**341–350

Sackin, H., Boulpaep, E.L. 1975. Models for coupling of salt and water transport. Proximal tubular reabsorption in *Necturus* kidney. *J. Gen. Physiol.* **66:**671–733

Spring, K.R. 1983. Fluid transport by gallbladder epithelium. *J. Exp. Biol.* **106:**181–194

Spring, K.R., Ericson, A.-C. 1982. Epithelial cell volume modulation and regulation. *J. Membrane Biol.* **69:**167–176

Spring, K.R., Hope, A. 1979. Fluid transport and the dimensions of cells and interspaces of living *Necturus* gallbladder. *J. Gen. Physiol.* **73:**287–305

Suzuki, K., Kottra, G., Kampmann, L., Frömter, E. 1982. Square wave pulse analysis of cellular and paracellular conductance pathways in *Necturus* gallbladder epithelium. *Pfluegers Arch.* **394:**302–312

Weinstein, A.M., Stephenson, J.L. 1981. Coupled water transport in standing gradient models of the lateral intercellular space. *Biophys. J.* **35:**167–191

Whitlock, R.T., Wheeler, H.O. 1964. Coupled transport of solute and water across rabbit gallbladder epithelium. *J. Clin. Invest.* **43:**2249–2265

Woessner, D.E. 1961. Nuclear transfer effects in nuclear magnetc resonance pulse experiments. *J. Chem. Phys.* **35:**41–48

Received 11 February 1985

Appendix

The simplest model for fluid transport across the gallbladder epithelium which takes account of the possibility of salt-water coupling in the interspace is depicted in Fig. 5. The main features are: (1) solute is transported across the apical membrane by an

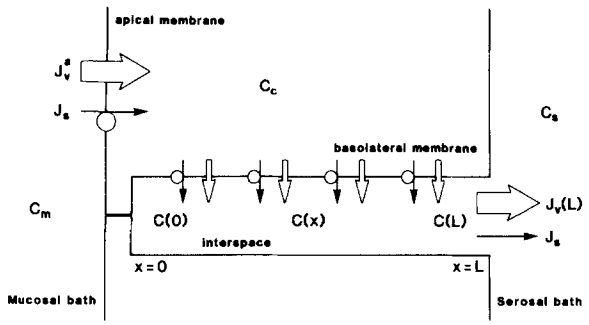

Fig. 5. A modified standing-gradient model for fluid transport across *Necturus* gallbladder epithelium, incorporating osmotic water flow across the apical membrane, and with salt transport uniformly distributed over the entire length of the interspace. Salt fluxes (J_s) and water fluxes (J_v) are represented by thin and thick arrows, respectively

unspecified mechanism and at a constant rate J_s; (2) solute transport at the same total rate is distributed uniformly over the basolateral membrane; and (3) water flow is assumed to be entirely transcellular and driven by osmosis across both the apical and the basolateral membranes.

Flow Equations

The flux of water across the apical membrane J_v^a will be given by

$$J_v^a = P_{os}^a(C_c - C_m) \tag{13}$$

where P_{os}^a is the effective osmotic permeability of the apical membrane, and C_c and C_m are the cell and mucosal bath osmolarities, respectively.

The well-known general equations for salt and water flow along the interspace (Diamond & Bossert, 1967; Hill, 1975) may be rewritten for the simpler case of uniformly distributed basolateral solute transport in the form

$$\frac{dJ_v}{dx} = 2lP_{os}^b \cdot (C(x) - C_c) \tag{14}$$

$$\frac{dC}{dx} = \frac{J_v(x) \cdot C(x) - J_s \cdot (x/L)}{Dwl} \tag{15}$$

where $J_v(x)$ and $C(x)$ are the longitudinal volume flux and osmolarity in the interspace at a distance x from the junctional end. L and w are the length and width of the interspace, and l is its linear extent in the plane of the epithelium. D is the diffusion coefficient of NaCl.

Table 2. Parameter values for 1 cm² of *Necturus* gallbladder epithelium[a]

J_s	$= 5 \times 10^{-10}$	osmole sec^{-1}
P_{os}^a	$= 8 \times 10^{-4}$	cm sec^{-1} osmolar^{-1}
P_{os}^b	$= 4 \times 10^{-4}$	cm sec^{-1} osmolar^{-1}
w	$= 0.5 \times 10^{-4}$	cm
L	$= 30 \times 10^{-4}$	cm
l	$= 1000$	cm
D	$= 1.5 \times 10^{-5}$	cm² sec^{-1}

[a] The values for J_s and the geometric parameters are based on data from Spring and Hope (1979) and Hill and Hill (1978).

The boundary conditions for the solution of Eqs. (14) and (15) are: (i) that the volume flux at the junctional end of the interspace is zero, i.e., $J_v(0) = 0$; and (ii) that, at the serosal end, the solute osmolarity in the interspace equals the serosal bath osmolarity, i.e. $C(L) = C_s$.

In order to obtain a steady-state solution, a value of C_c is sought where the volume flux leaving the interspace equals the volume flux across the apical membrane predicted by Eq. (13). The osmolarity of the absorbate is then given by

$$C_a = J_s/J_v(L). \tag{16}$$

Numerical Solutions

By a simple numerical method, using the parameter values given in Table 2, solutions have been obtained for the following realistic situations:

(a) *Unilateral Preparation*
C_m is set at 200 mosmolar and the absorbate is allowed to form the serosal bath. Thus $C(L) = C_s = C_a = J_s/J_v(L)$. The value of C_a predicted by the model is 204.1 mosmolar, and $J_v(L)$ is 8.8 μl cm^{-2} hr^{-1}. C_c is 203.1 mosmolar.

(b) *Symmetrical Solutions*
C_m and C_s are both set at 200 mosmolar. In the steady state, the predicted value of C_a is 1602 mosmolar, $J_v(L)$ is 1.1 μl cm^{-2} hr^{-1} and C_c is 200.4 mosmolar.

(c) *Strength of Transport*
C_s is set at 200 mosmolar and C_m is progressively raised until a solution is found where $J_v(L) = 0$. The value of C_m at which this is achieved is 200.6 mosmolar.